nature communications

Article

https://doi.org/10.1038/s41467-025-59817-9

Persistent acyclic Cp*Ir(III) complexes and their reactivities in cross-coupling reactions

Received: 25 March 2025

Accepted: 6 May 2025

Published online: 15 May 2025

Check for updates

Yimin Wu, Yayin Deng, Guangying Tan & Jingsong You

Iridium(III) complexes play a prominent role in organometallic chemistry, with significant research efforts directed toward Cp*Ir(III) species, broadly categorized into cyclic and acyclic types. Although studies on these two classes began roughly simultaneously, the development of acyclic Cp*Ir(III) complexes has lagged significantly behind their cyclic counterparts. Herein, we report a general and efficient strategy for synthesizing various persistent aryl Cp*Ir(III)(CO)Cl complexes directly from aryl aldehydes, with in situ generated CO as a stabilizing ligand. These acyclic Cp*Ir(III) complexes showcase exceptional reactivity, undergoing reactions with up to eight classes of nucleophiles to generate diverse diorganoiridium(III) species with remarkable stability. Electrochemical analysis of these complexes provides insights into their reductive elimination processes. Guided by these findings, Cp*Ir(III)-mediated decarbonylative C–C and C–O cross-couplings of aryl aldehydes are successfully developed. This study establishes a robust platform for the exploration of acyclic Cp*Ir(III) complexes, paving the way for further advancements in iridium(III) chemistry.

Iridium(III) chemistry represents a fundamental and dynamic field within organometallic chemistry, attracting substantial research interest over the decades. The synthesis and characterization of the dimeric complex $[Cp^*IrCl_2]_2$ by Maitlis and coworkers in 1969 marked a pivotal milestone[1], sparking extensive investigations into related half-sandwich organoiridium(III) complexes (Fig. 1a). Subsequently, in 1985, the same group successfully prepared and isolated a cyclometallated Cp*Ir(III) complex from benzoic acid using a chelation strategy[2]. Since then, numerous kinetically stable cyclometallated Cp*Ir(III) complexes have been synthesized and characterized[3,4]. These complexes have played crucial roles in stoichiometric organometallic transformations and have found wide-ranging catalytic applications (Fig. 1a, left)[5–13]. Today, cyclometallated Cp*Ir(III) complexes are recognized for their remarkable catalytic efficiency in diverse reactions, including asymmetric hydrogenation, dehydrogenative oxidation, hydrosilylation, and C–H functionalization[14–25].

Research on acyclic Cp*Ir(III) complexes has advanced at a slower pace compared to their cyclic counterparts, despite early investigations dating back to the 1970s (Fig. 1a, right). In 1971, Maitlis demonstrated the reduction of $[Cp^*IrCl_2]_2$ with CO gas to yield $Cp^*Ir(CO)_2$, which, upon treatment with arylsulfonyl chloride at 110 °C, released SO_2 to produce aryl Cp*Ir(CO)Cl complexes. However, the reactivity of these organoiridium(III) complexes was not further explored[26]. Later, Bergman reported the synthesis of a highly reactive $Cp^*(PMe_3)IrH_2$ complex via successive treatment of $[Cp^*IrCl_2]_2$ with PMe_3 and $LiEt_3BH$. This complex was shown to activate C–H bonds in benzene, cyclohexane, and neopentane stoichiometrically under UV irradiation, producing three air-sensitive aryl/alkane $Cp^*Ir(III)(PMe_3)H$ complexes[27]. Despite these pioneering efforts, subsequent studies on acyclic Cp*Ir(III) complexes have remained limited, predominantly focusing on their synthesis and structural characterization. These endeavors often rely on the use of exogenous ligands and intricate multi-step synthetic procedures[28–32]. Unlike their cyclic counterparts, the reduced structural rigidity of acyclic Cp*Ir(III) complexes renders them more fragile, which limits their accessibility and practical applications[33–36]. As a result, studies exploring their stoichiometric reactivity and catalytic potential have been sparse[37–40]. To advance the field of iridium(III) chemistry, it is highly desirable to develop straightforward and efficient methods for

Key Laboratory of Green Chemistry and Technology of Ministry of Education, College of Chemistry, Sichuan University, Chengdu 610064, People's Republic of China. e-mail: guangying@scu.edu.cn; jsyou@scu.edu.cn

https://doi.org/10.1038/s41467-025-59817-9

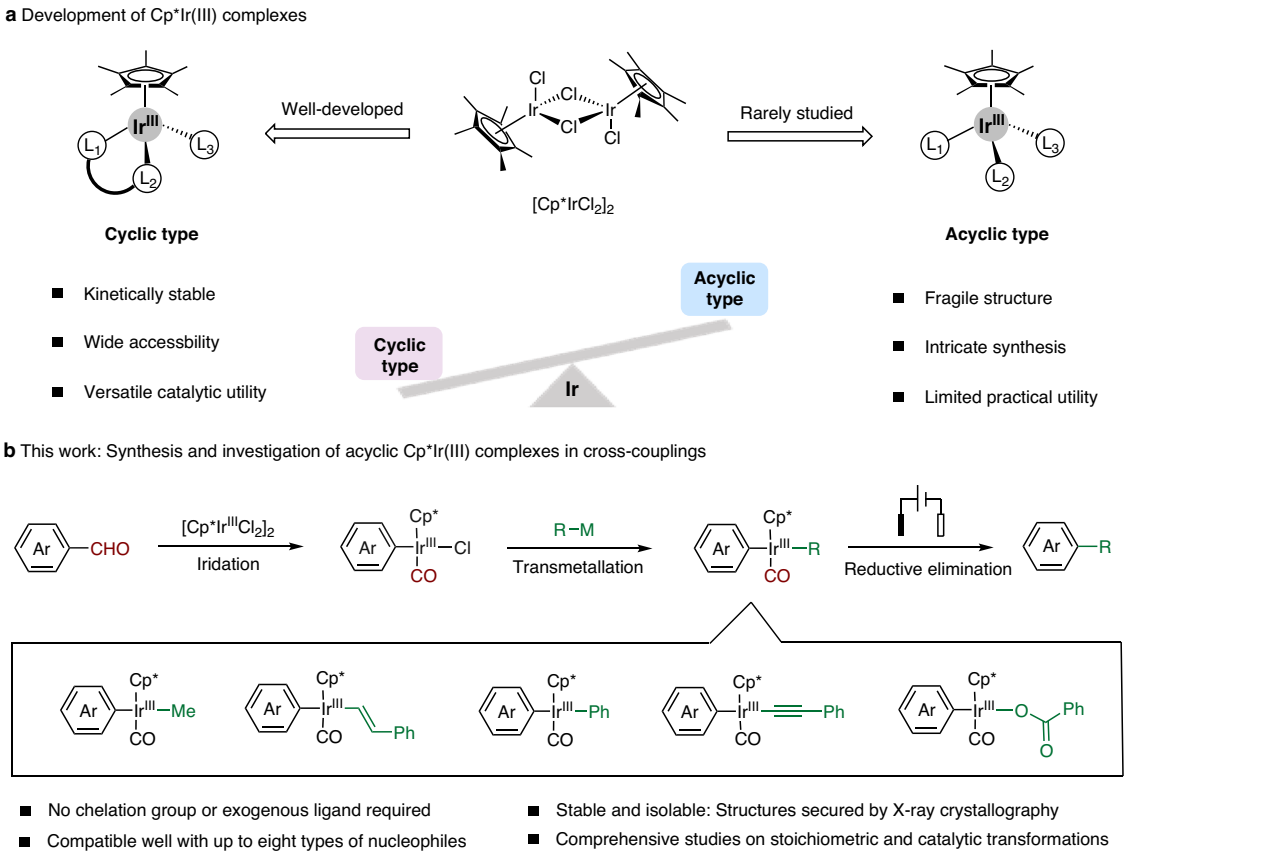

Fig. 1 | Context of the work. a Development of Cp*Ir(III) complex. **b** This work: synthesis and investigation of acyclic Cp*Ir(III) complexes in cross-couplings. Cp* pentamethylcyclopentadienyl, Me methyl, Ph phenyl.

synthesizing acyclic Cp*Ir(III) complexes with enhanced stability, ideally starting from simple feedstocks. Such efforts would facilitate a deeper understanding of their chemical properties and broaden their potential applications.

Herein, we report a general method for synthesizing a diverse array of acyclic Cp*Ir(III) complexes directly from readily available aryl aldehydes, along with an investigation of their chemical reactivity (Fig. 1b). In this approach, aryl aldehydes undergo direct iridation with $[Cp^*IrCl_2]_2$ to provide aryl Cp*Ir(III)(CO)Cl species. The in situ generated CO serves as a coordinating ligand, stabilizing these acyclic species and obviating the need for chelating groups or exogenous ligands. These isolable aryl Cp*Ir(III)(CO)Cl complexes then undergo transmetallation, demonstrating broad compatibility with eight distinct nucleophiles. The resulting post-transmetallation diorganoiridium(III) species, including aryl–Ir–aryl, aryl–Ir–alkenyl, aryl–Ir–alkynyl, aryl–Ir–alkyl, and aryl–Ir–acyloxy complexes, exhibit exceptional air and moisture stability. Electrochemical studies of these diorganoiridium(III) complexes reveal oxidation potentials that guide reductive elimination processes, implicating an Ir(IV) intermediate in the reaction mechanism. Building on these insights, we developed Cp*Ir(III)-mediated and -catalyzed C–C and C–O cross-coupling reactions. Collectively, this work establishes a versatile platform for probing the fundamental stoichiometric chemical processes of iridium-enabled cross-couplings and provides a foundation for advancing Ir(III)-catalyzed cross-coupling methodologies.

Results

Iridation

This work was initiated by an unexpected discovery made during our investigation into the mechanism of iridium-catalyzed *ortho* C–H activation of benzaldehyde[41]. Our original aim was to synthesize a carbonyl-chelated iridacycle by treating benzaldehyde (**1a**) with $[Cp^*IrCl_2]_2$ in the presence of NaOAc in 1,2-dichloroethane (DCE). To our surprise, the reaction did not yield the anticipated iridacycle. Instead, we isolated an acyclic phenyl Cp*Ir(III)(CO)Cl complex, **3a**. We hypothesize that the formation mechanism of this species involves a tandem C–H activation and CO deinsertion process from **1a**, where the in situ generated CO behaves as a stabilizing ligand, negating the need for an external ligand (Fig. 2a). Systematic optimization of the reaction conditions led to the successful synthesis of **3a** in a 52% yield (for details see Table S1).

With the optimized reaction conditions established, we explored the substrate scope of aryl aldehydes. As depicted in Fig. 2b, a wide variety of aryl aldehydes (**1**) reacted with $[Cp^*IrCl_2]_2$ to provide aryl Cp*Ir(III)(CO)Cl complexes in moderate yields. Aryl aldehydes bearing either electron-donating or electron-withdrawing substituents on the phenyl ring were well-tolerated, yielding the corresponding complexes **3a**–**3s**. This reaction exhibited exclusive selectivity and accommodated a plethora of sensitive functional groups, including chloro, bromo, iodine, methoxy, acyloxy, ester, amide, nitro, cyano, and *N*-morpholino groups. This broad functional group tolerance likely arises from the intrinsic properties of iridium-mediated C–H activation. Furthermore, multisubstituted benzaldehydes and naphthaldehydes also participated in this transformation under the optimized conditions (**3t**–**3w**). The reaction of $[Cp^*IrCl_2]_2$ with cinnamaldehyde or hexanal failed to undergo iridation (see Supplementary Information for the details, Fig. S2). All aryl Cp*Ir(III)(CO)Cl complexes were readily purified via silica gel column chromatography and exhibited robust stability in both air and moisture, enabling their comprehensive characterization and further investigation of their properties.

The structures of selected aryl Cp*Ir(III)(CO)Cl complexes (**3d, 3e, 3f, 3i, 3l**, and **3w**) were elucidated by single-crystal X-ray diffraction. As depicted in Fig. 2c, the coordination environment surrounding the Ir

https://doi.org/10.1038/s41467-025-59817-9

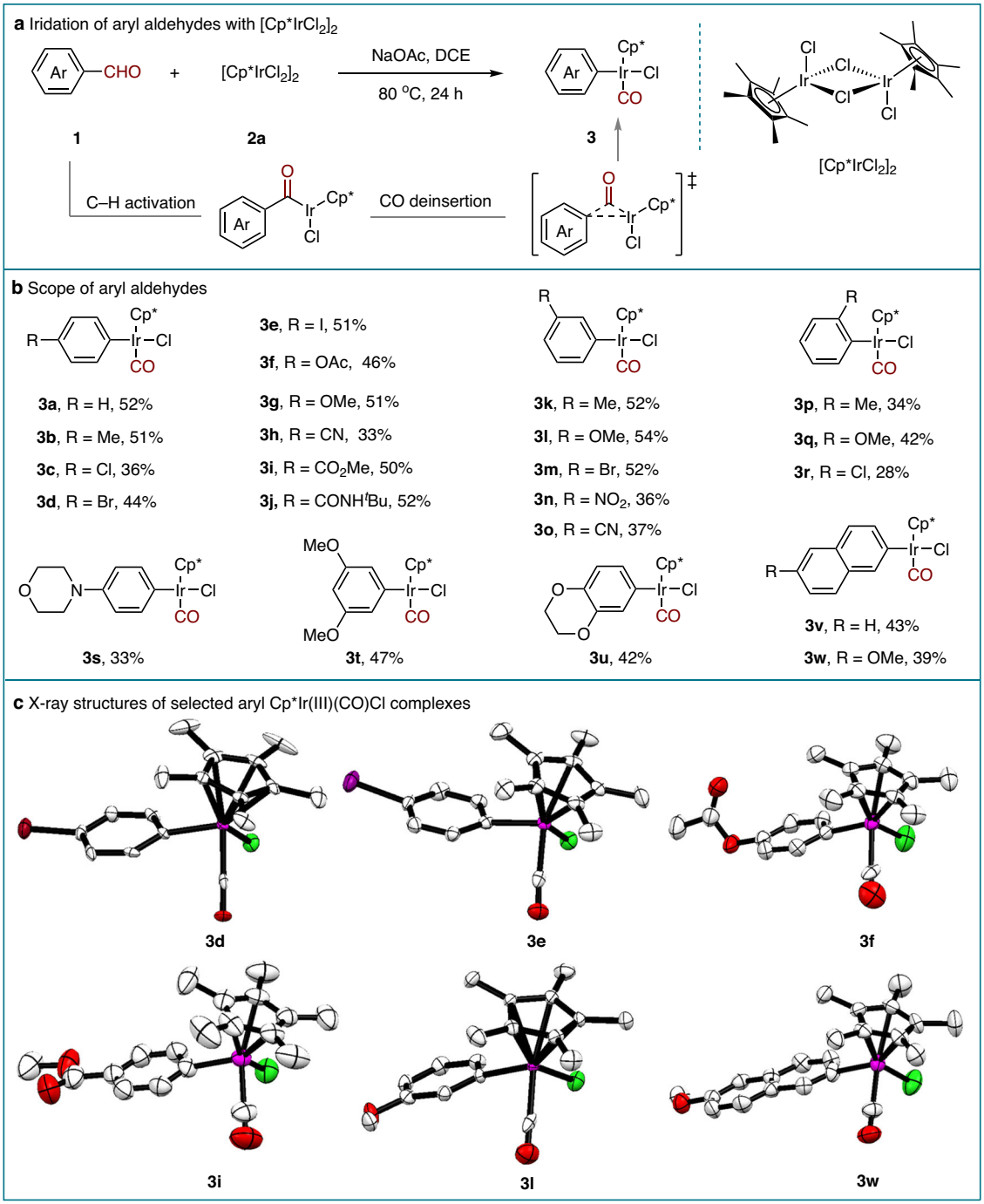

Fig. 2 | Iridation of aryl aldehydes. a Iridation of aryl aldehydes with $[Cp^*IrCl_2]_2$. **b** Scope of aryl aldehydes. Reaction conditions: Aldehyde **1** (0.40 mmol), $[Cp^*IrCl_2]_2$ (0.05 mmol) and NaOAc (1.0 mmol) in DCE (1.0 mL) under N_2 at 80 °C for 24 h. Isolated yields are given. **c** X-ray structures of selected aryl Cp*Ir(III)(CO)Cl complexes. Cp* pentamethylcyclopentadienyl, Me methyl, ^{t}Bu *tert*-butyl, DCE 1,2-dichloroethane.

center consists of an η^5-Cp* ligand, a chloride ion, a carbonyl ligand, and an aryl group. This structural arrangement confirms that the oxidation state of the Ir center remains unaltered following the iridation procedure, which occurs via a concerted metallation–deprotonation (CMD) mechanism[42]. This pathway contrasts with the traditional oxidation addition typically involved in low-valent metal-mediated decarbonylation processes[43]. In these complexes, the Ir–Cl bond lengths range from 2.3687(16) to 2.3885(18) Å, while the Ir–C(ipso) bond lengths span 2.075(7) to 2.098(7) Å (Table S19). The Ir–CO bond distances (1.862(10) to 1.982(6) Å) are shorter than those of the Ir–C(Ar) bonds, indicating a relatively strong coordination between the Ir center and the CO ligand. This strong Ir–CO interaction likely contributes to the notable stability of these complexes. Additionally, the C(Ar)–Ir–Cl angles are approximately 90°, consistent with a pseudo-tetrahedral geometry[44]. These structural insights provide valuable additions to the growing database of Ir(III) complexes and enhance our understanding of their coordination chemistry.

Transmetallation

The transmetallation step, a pivotal stage in cross-coupling reactions, entails the migration of an organic group from one metal to another and is heavily influenced by the choice of nucleophile[45,46]. Despite its significance, the capture and characterization of post-transmetallation organoiridium species remain underexplored, with limited reports in

https://doi.org/10.1038/s41467-025-59817-9

the literature. In this study, the successful synthesis of aryl Cp*Ir(III)(CO)Cl complexes offers a unique opportunity to probe this mechanism. As shown in Fig. 3, these stable complexes served as robust platforms for transmetallation, enabling the isolation of a broad range of diorganoiridium species. Surprisingly, this reaction exhibited compatibility with eight distinct classes of nucleophiles, encompassing

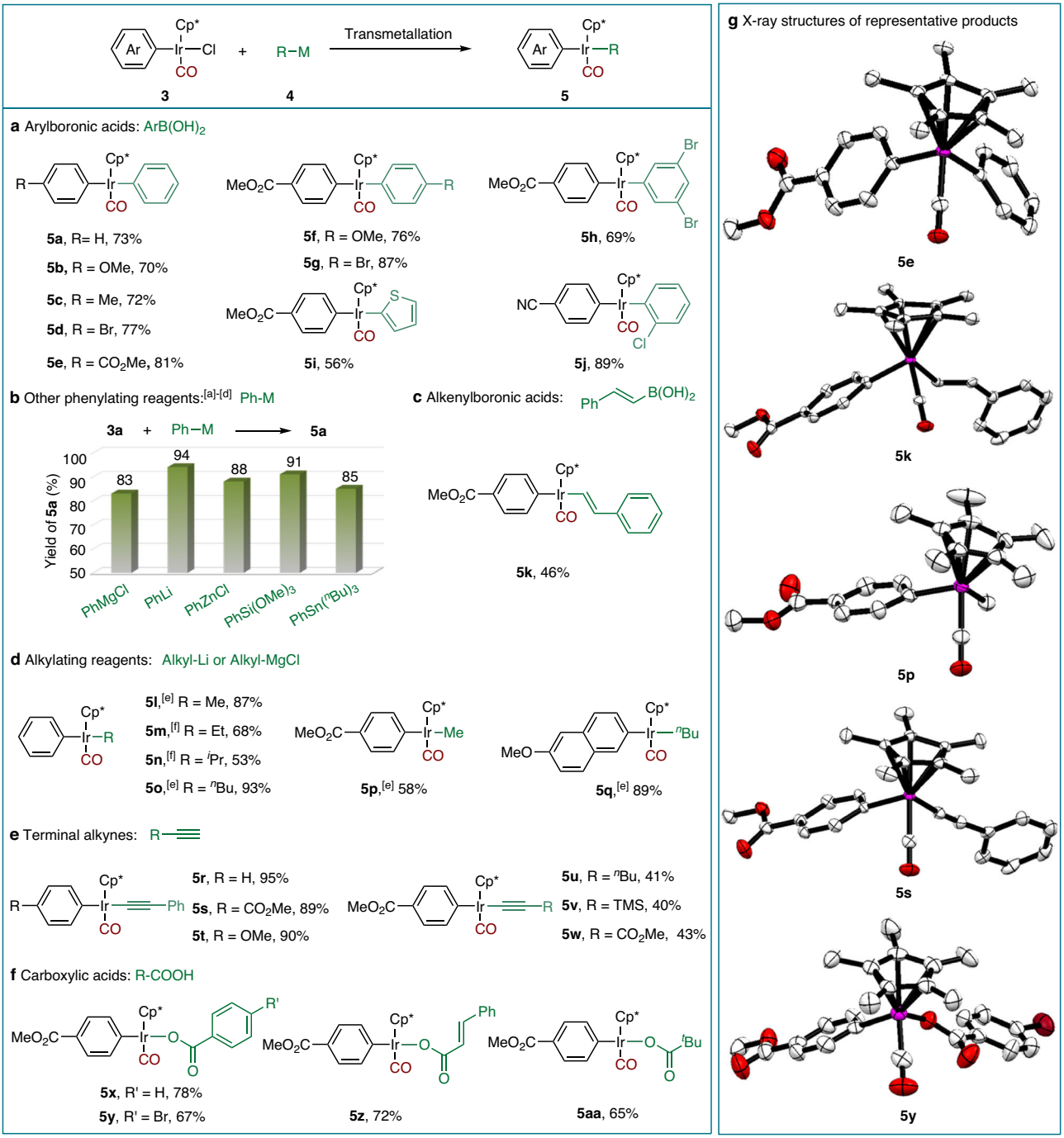

Fig. 3 | Transmetallation of aryl Cp*Ir(III)(CO)Cl complexes with diverse nucleophiles. a Transmetallation with arylboronic acids. Reaction conditions: Aryl Cp*Ir(III)(CO)Cl complex (0.10 mmol), arylboronic acid (0.40 mmol) and K_2CO_3 (0.40 mmol) in toluene (1.0 mL) under N_2 at 80 °C for 24 h. **b** Transmetallation with other phenylating reagents. Reaction conditions: [a]**3a** (0.10 mmol) and PhMgCl or PhLi (0.15 mmol) in THF (1.0 mL) under N_2 at room temperature for 3 h. [b]**3a** (0.10 mmol) and PhZnCl (0.15 mmol) in THF (1.0 mL) under N_2 at 60 °C for 10 h. [c]**3a** (0.10 mmol), $Cu(OAc)_2$ (0.01 mmol), $^nBu_4NF$ (0.30 mmol) and $PhSi(OMe)_3$ (0.15 mmol) in THF (1.0 mL) under N_2 at room temperature for 24 h. [d]**3a** (0.10 mmol) and $PhSn(^nBu)_3$ (0.20 mmol) in toluene (1.0 mL) under N_2 at 120 °C for 24 h. **c** Transmetallation with alkenylboronic acid. Reaction conditions: Aryl Cp*Ir(III)(CO)Cl complex (0.10 mmol), alkenylboronic acid (0.40 mmol) and K_2CO_3 (0.40 mmol) in toluene (1.0 mL) under N_2 at 65 °C for 24 h. **d** Transmetallation with alkylating reagents. Reaction conditions: [e]Aryl Cp*Ir(III)(CO)Cl complex (0.10 mmol) and alkyl−Li (0.15 mmol) in THF (1.0 mL) under N_2 at −60 °C for 0.5 h. [f]Aryl Cp*Ir(III)(CO)Cl complex (0.10 mmol) and alkyl−MgCl (0.15 mmol) in THF (1.0 mL) under N_2 at 0 °C for 5 min. **e** Transmetallation with terminal alkynes. Reaction conditions: Aryl Cp*Ir(III)(CO)Cl complex (0.10 mmol), terminal alkyne (0.30 mmol), CuCl (0.005 mmol) and NEt_3 (0.30 mmol) in THF (1.0 mL) under N_2 at 80 °C for 24 h. **f** Transmetallation with carboxylic acids. Reaction conditions: Aryl Cp*Ir(III)(CO)Cl complex (0.10 mmol), carboxylic acid (0.30 mmol) and Ag_2O (0.15 mmol) in DCE (1.0 mL) under N_2 at 80 °C for 24 h. **g** X-ray structures of representative products. Cp* pentamethylcyclopentadienyl, Me methyl, Ph phenyl, Et ethyl, ^{i}Pr *iso*-propyl, ^{n}Bu *n*-butyl, TMS trimethylsilyl, ^{t}Bu *tert*-butyl, THF tetrahydrofuran, DCE 1,2-dichloroethane.

aryl/alkenyl boronic acids, aryl/alkyl magnesium reagents, aryl/alkyl lithium reagents, arylzinc reagents, arylsilanes, aryltin reagents, alkynes, and even carboxylic acids. For instance, arylboronic acids underwent smooth transmetallation with aryl Cp*Ir(III)(CO)Cl complexes in the presence of K_2CO_3 in toluene under N_2 at 80 °C, yielding aryl–Ir–aryl complexes (**5a**–**5j**) with excellent functional group compatibility (Fig. 3a). Similarly, a range of organometallic arylating reagents, including PhMgCl, PhLi, PhZnCl, $PhSi(OMe)_3$ and $PhSn(^nBu)_3$, reacted effectively with complex **3a** to afford complex **5a** in high yields (Fig. 3b). (*E*)-Styrylboronic acid also participated in this transformation, yielding the corresponding aryl–Ir–alkenyl complex (**5k**) in a 46% yield while preserving the *trans* configuration of the alkene (Fig. 3c). Organometallic alkylating reagents, such as alkyl–Li and alkyl–MgCl, were similarly effective, forming aryl–Ir–alkyl complexes (**5l**–**5q**) in moderate to good yields (Fig. 3d). Unexpectedly, terminal alkynes underwent efficient transmetallation with aryl Cp*Ir(III)(CO)Cl complexes in the presence of triethylamine as the base and CuCl as the catalyst, furnishing diverse aryl–Ir–alkynyl complexes (**5r**–**5w**, Fig. 3e). This process likely involves the initial formation of an alkynyl copper intermediate[47], which transmetallates with aryl Cp*Ir(III)(CO)Cl complex (see Supplementary Information for the details, Section IV). To further explore the scope, non-carbon-based nucleophiles, such as carboxylic acids, were examined. Aryl, alkenyl, and alkyl carboxylic acids successfully underwent transmetallation to generate aryl–Ir–acyloxy complexes (**5x**–**5aa**) in satisfactory yields (Fig. 3f). When employing phenol or aniline as nucleophile, no target product was observed (see Supplementary Information for the details, section IV). Collectively, these results underscore the remarkable versatility of aryl Cp*Ir(III)(CO)Cl complexes in accessing diverse diorganoiridium species, providing valuable intermediates for mechanistic studies and further applications, which have previously been difficult to achieve.

To illustrate the structural characteristics of these complexes, single crystal X-ray diffraction analyses were conducted on each type of diorganoiridium complexes (**5e, 5k, 5p, 5s**, and **5y**) (Fig. 3g, Tables S13–S17 and S20). In these complexes, the Ir–C bond lengths between the iridium center and the carbon atom of the original aryl group or CO ligand range from 2.064(4) to 2.088(9) Å and 1.826(12) to 1.863(4) Å, respectively, slightly shorter than the corresponding bonds in their chloride precursors. The Ir–C(Nu) bond lengths of the newly formed bonds vary depending on the hybridization of the carbon atoms in the nucleophiles, ranging from 1.999(4) to 2.106(9) Å. Notably, the Ir–C(alkynyl) bond is the shortest at 1.999(4) Å, while the Ir –alkyl bond is the longest at 2.106(9) Å. The Ir–C(aryl) and Ir–C(alkenyl) bonds fall in between, measuring 2.076(4) and 2.072(5) Å, respectively. Additionally, the Ir–O bond in complex **5y** is 2.072(7) Å, closely resembling the Ir–C(alkenyl) bond length in complex **5k**. The bond angles, specifically the C(Ar)–Ir–C(Nu) or O(Nu) angles, are smaller than those observed in their chloride counterparts, likely due to increased steric hindrance in the diorganoiridium species. These diorganoiridium complexes, which were previously difficult to access or required elaborate synthetic efforts, represent a significant advancement and offering valuable opportunities to investigate elementary steps in Cp*Ir(III)-enabled cross-coupling reactions.

Reductive elimination

The catalytic cycle concludes with reductive elimination, a key step in which two bonds are broken and a new bond is formed between two organic groups[48]. In traditional transition metal-catalyzed cross-coupling reactions, especially those involving palladium, C–C bond formation typically proceeds through transmetallation followed by direct reductive elimination[49–63]. However, attempts to achieve direct reductive elimination from the synthesized diorganoiridium complexes were unsuccessful, implying that their high kinetic stability impedes the formation of the desired cross-coupling products. To address this limitation, we hypothesized an alternative high-valent pathway wherein the post-transmetallation species is activated via oxidation of the metal center, thereby facilitating the reductive elimination process[64]. To verify this hypothesis, cyclic voltammetry (CV) experiments were conducted to examine the redox behavior of the aryl–Ir–aryl complexes. The cyclic voltammograms of five electronically varied aryl–Ir–aryl complexes displayed two irreversible redox events, tentatively assigned to the Ir(III)/Ir(IV) redox couple ($E_1^{Ox}{}_{p/2}$) and the oxidation of Ir(IV) to Ir(V) ($E_2^{Ox}{}_{p/2}$), respectively (Fig. 4a)[65]. Hammett plot analysis of the half peak oxidation potential ($E^{Ox}{}_{p/2}$) revealed positive Hammett-slopes (ρ), indicating that electron-donating substituents facilitate the electro-oxidation process, whereas electron-withdrawing substituents reduce the electron density at the iridium center, thereby increasing the oxidation potential (Fig. 4b, c)[66]. The reduction peaks further corroborated the electronic influence of the aryl ligands, confirming the role of substituent effects in modulating redox behavior (Fig. 4d, e). The peak positions of both redox events depend on the scan rate, implying an electrochemical-chemical (EC) mechanism[67–69]. For instance, as the scan rate increased from 50 to 400 mV s^{-1}, the electrochemical response current of **5d** intensified, while the CV profiles maintained consistent, displaying only minor shifts in peak positions (Fig. 4f).

Building on the characterization of the redox behaviors of the aryl–Ir–aryl complexes, we proceeded with the reductive elimination of the post-transmetallation complexes through an electrochemical pathway. Unlike traditional chemical oxidation methods, which often necessitate the careful selection of oxidizing agents and can be time-consuming, organic electrochemistry offers precise control of reaction voltage or current, tailored to the redox potential of the reactants. This approach is both sustainable and environmentally friendly, making it an attractive alternative[70–75]. Additionally, insights from electrochemical oxidation experiments can inform chemical oxidation strategies. In this study, electrolysis of aryl–Ir–aryl complex **5e** ($E_1^{Ox}{}_{p/2}$ = 1.18 V, $E_2^{Ox}{}_{p/2}$ = 2.11 V vs saturated calomel electrode (SCE) in MeCN) was performed in a $^nBu_4NPF_6$ electrolyte solution, resulting in reductive elimination and the formation of the desired C–C coupled product **6a** (Fig. 4g). Systematic variation of electrical current and potential provided further insight into this reaction. At a constant current of 5 mA, the yield of **6a** peaked at 70%, with deviations in current intensity leading to reduced yields. Notably, reductive elimination did not occur at an applied voltage of 1.0 V ($U_{a,i} \approx 0.8$ V vs SCE in MeCN), which is below the $E_1^{Ox}{}_{p/2}$ of **5e**. Moreover, applying an anodic potential slightly above the $E_1^{Ox}{}_{p/2}$ of **5e** (U_{cell} = 3.0 V, $E_{a,i} \approx 1.2$ V vs SCE in MeCN) (Differences exist between the input potential of the electrolysis cell and the real anodic potential, and the initial anodic potentials were measured by a three-electrode system. In this three-electrode system, Ag/Ag^+, platinum wire and the anodic of the electrolysis cell serve as reference, counter and work electrode, respectively. The real anodic potential is the potential between the reference electrode and the anodic.) generated **6a** in a yield of 32%, implying that the electrochemical reductive elimination occurs via a high-valent Cp*Ir(IV) intermediate, as the applied voltage was insufficient to oxidize the Ir(III) intermediate to Ir(V). Increasing the potential further to 4.0 V ($E_{a,i} \approx 1.7$ V vs SCE in MeCN) reduced the yield to 27% yield, presumably due to competing decomposition pathways from over-oxidation. To complement the electrochemical studies, the oxidation-induced reductive elimination of **5e** at room temperature was examined using chemical oxidants, including AgOAc, AgOTFA, DDQ (2,3-dichloro-5,6-dicyano-1,4-benzoquinone), and $NOPF_6$ (Fig. 4h)[76]. As expected, oxidants with lower redox potentials, such as Ag(I) salts ($E_{p/2}$ = 0.44 V vs SCE in MeCN) and DDQ ($E_{p/2}$ = 0.53 V vs SCE in MeCN), failed to promote reductive elimination. In contrast, $NOPF_6$ ($E_{p/2}$ = 1.27 V vs SCE in MeCN), with a sufficiently high redox potential, effectively facilitated reductive elimination, consistent with the

https://doi.org/10.1038/s41467-025-59817-9

electrochemical findings. Using 1.0 equiv. of $NOPF_6$ afforded **6a** in a 64% yield, further supporting the hypothesis that the reductive elimination is induced by single-electron oxidation.

The successful electrochemical reductive elimination of **5e** led us to investigate whether other types of post-transmetallation diorganoiridium complexes could similarly undergo reductive elimination.

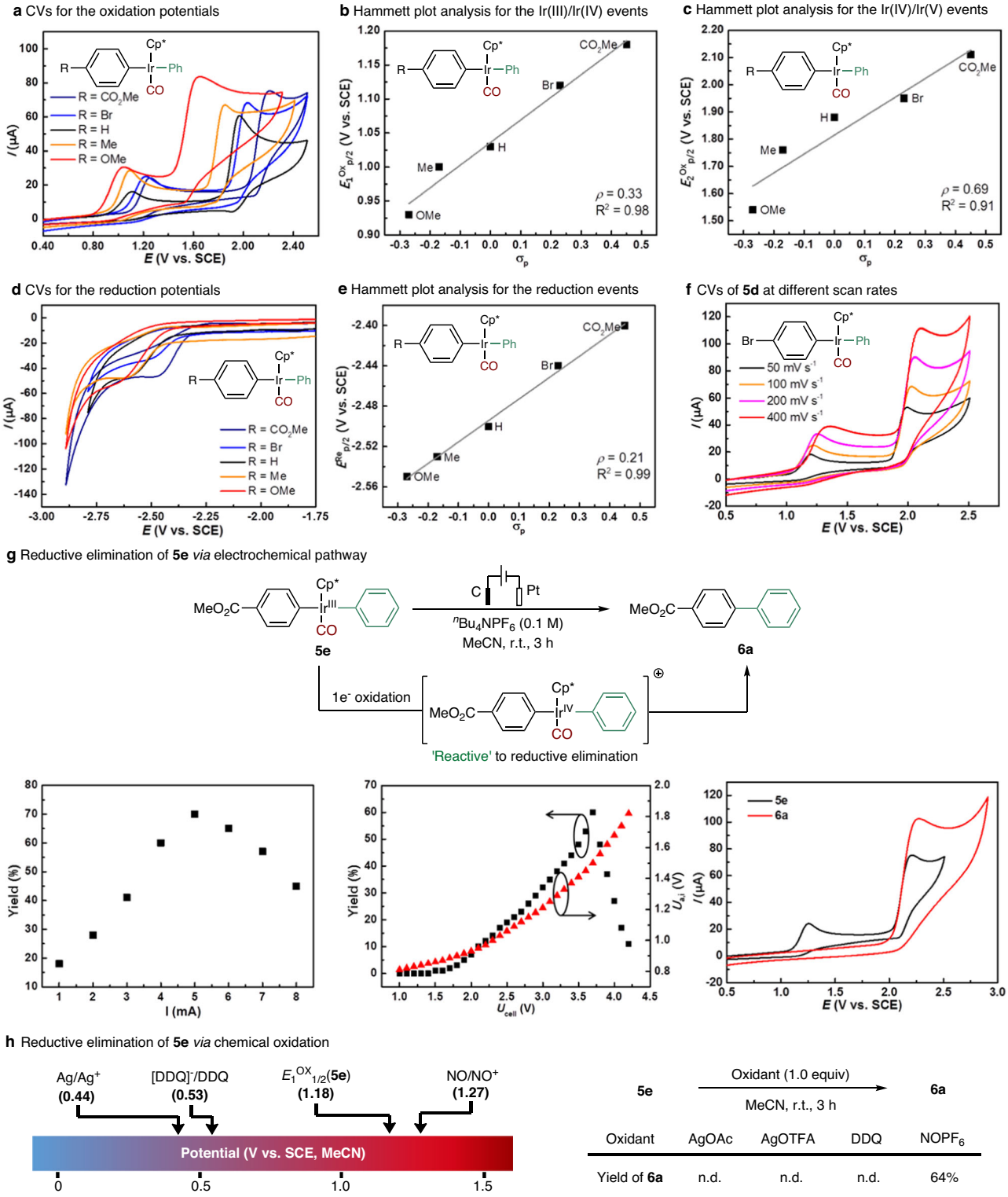

Fig. 4 | Electrochemical analysis and reductive elimination of aryl-Ir(III)-aryl species. a CVs for the oxidation potentials (0.1 M $^nBu_4NPF_6$ in MeCN, 100 mV s^{-1}). **b** Hammett plot analysis for the Ir(III)/Ir(IV) events. **c** Hammett plot analysis for the Ir(IV)/Ir(V) events. **d** CVs for the reduction potentials (0.1 M $^nBu_4NPF_6$ in MeCN, 100 mV s^{-1}). **e** Hammett plot analysis for the reduction events. **f** CVs of **5d** at different scan rates (0.1 M $^nBu_4NPF_6$ in MeCN). **g** Reductive elimination of **5e** via electrochemical pathway. Reaction conditions: with constant current or cell voltage, **5e** (0.10 mmol) and $^nBu_4NPF_6$ (0.50 mmol) in MeCN (5.0 mL) under N_2 at room temperature for 3 h (U_{cell}: Cell voltage; $U_{a,i}$: Initial anodic potential). **h** Reductive elimination of **5e** *via* chemical oxidation. Reaction conditions: **5e** (0.10 mmol) and oxidant (0.10 mmol) in MeCN (1.0 mL) under N_2 at room temperature for 3 h. Cp* pentamethylcyclopentadienyl, Me methyl, Ph phenyl, ^{n}Bu *n*-butyl, DDQ 2,3-dichloro-5,6-dicyano-1,4-benzoquinone.

https://doi.org/10.1038/s41467-025-59817-9

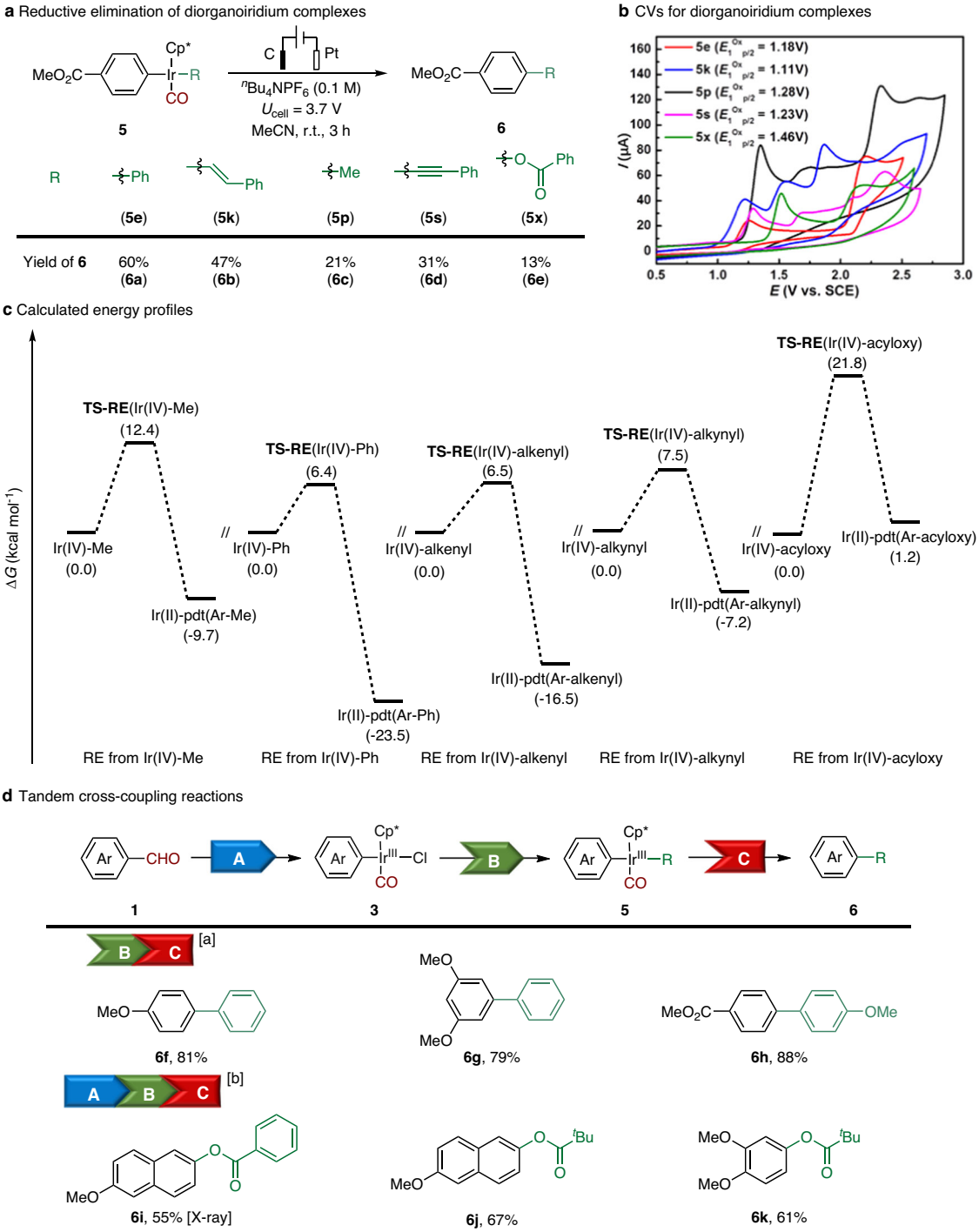

Fig. 5 | Investigation for the reductive elimination of diorganoiridium complexes and elementary steps-cascaded cross-coupling reaction. a Reductive elimination of diorganoiridium complexes. Reaction conditions: with a cell voltage of 3.7 V, diorganoiridium complex (0.10 mmol) and $^{n}Bu_4NPF_6$ (0.50 mmol) in MeCN (5.0 mL) under N_2 at room temperature for 3 h. **b** CVs for diorganoiridium complex (0.1 M $^{n}Bu_4NPF_6$ in MeCN, 100 mV s^{-1}). **c** Calculated energy profiles. **d** Tandem cross-coupling reactions. Reaction conditions: [a]Aryl Cp*Ir(III)(CO)Cl complex (0.10 mmol), arylboronic acid (0.40 mmol), AgOAc (0.10 mmol) and K_2CO_3 (0.40 mmol) in TFE (1.0 mL) under N_2 at 80 °C for 24 h. [b]Aryl aldehyde (0.20 mmol), carboxylic acid (0.40 mmol), $[Cp^*IrCl_2]_2$ (0.01 mmol), $AgNTf_2$ (0.04 mmol), Ag_2O (0.40 mmol) and NaOAc (0.20 mmol) in DCE (1.0 mL) under N_2 at 130 °C for 24 h. Cp* pentamethylcyclopentadienyl, Me methyl, Ph phenyl, ^{n}Bu *n*-butyl, TFE 2,2,2-Trifluoroethanol, DCE 1,2-dichloroethane.

As anticipated, all the diorganoiridium complexes, including aryl–Ir–alkenyl, aryl–Ir–alkyl, aryl–Ir–alkynyl, and aryl–Ir–acyloxy complexes (**5k, 5p, 5s**, and **5x**), smoothly underwent reductive elimination under electrochemical conditions, validating the oxidation strategy as a general approach for facilitating reductive elimination of post-transmetallation organoiridium complexes. To compare the reactivity of different types of complexes, their reductive elimination reactions were conducted at a constant electrolysis potential. As shown in Fig. 5a, the yields of the reductive elimination products followed a decreasing trend from **6a** to **6e**. This trend was hypothesized to arise

from variations in the redox properties of these diorganoiridium complexes. To test this hypothesis, CV measurements were performed to evaluate the redox potentials of these species. As outlined in Fig. 5b, the $E_1^{Ox}{}_{p/2}$ of **5e, 5k, 5p, 5s**, and **5x** were determined as 1.18, 1.11, 1.28, 1.23, 1.46 V *vs* SCE in MeCN, respectively, revealing an overall increasing trend. Since higher oxidation potentials indicate greater resistance to oxidation under a constant electrode potential, the observed fluctuation in yields of **6a** to **6e** can be logically attributed to the rising redox potentials of the complexes. This finding highlights the critical role of understanding the redox behavior of post-transmetallation diorganoiridium complexes for the optimization of reductive elimination.

To gain deeper insight into these results, density functional theory (DFT) calculations were performed. Experimental evidence established that oxidation-induced reductive elimination occurs from a high-valent Ir(IV) intermediate rather than Ir(V). Accordingly, the DFT calculations focused on the reductive elimination pathways originating from the Ir(IV) intermediates. As illustrated in Fig. 5c, the reductive elimination from the aryl–Ir(IV)–alkyl, aryl–Ir(IV)–aryl, aryl–Ir(IV)–alkenyl, and aryl–Ir(IV)–alkynyl intermediates is energetically downhill by 9.7, 23.5, 16.5, and 7.2 kcal mol^{-1}, respectively, with barriers ranging from 6.4 to 12.4 kcal mol^{-1}. Conversely, reductive elimination from the aryl–Ir(IV)–acyloxy intermediate exhibits a significantly higher barrier of 21.8 kcal mol^{-1} and is energetically uphill by 1.2 kcal mol^{-1}. This elevated energy barrier likely accounts for the reduced efficiency of reductive elimination for aryl–Ir–acyloxy complexes compared to other types of diorganoiridium species under a constant electrode potential (Fig. 5a).

Stoichiometric and catalytic reactions

Based on the stoichiometric reactivity of these organoiridium complexes, we further investigated the feasibility of cascade reactions. To our delight, tandem transmetallation and reductive elimination of aryl Cp*Ir(III)(CO)Cl complexes with aryl boronic acids were successfully achieved in the presence of K_2CO_3 and AgOAc in 2,2,2-trifluoroethanol at 80 °C, producing the corresponding C – C cross-coupled products (**6f**–**6 h**) in good yields. Furthermore, although the energy barrier of the reductive elimination from aryl-Ir(IV)-acyloxy intermediate is up to 21.8 kcal mol^{-1}, a catalytic version of the Cp*Ir-enabled decarbonylative cross-coupling reaction was developed for aryl aldehydes and carboxylic acids under elevated temperature conditions. Using Ag_2O as a chemical oxidant, aryl aldehydes were effectively coupled with aryl or alkyl carboxylic acids under iridium catalysis at 130 °C, yielding the desired C–O cross-coupled products (**6i**–**6k**) in moderate yields (Fig. 5d). These findings underscore the versatility of the aryl Cp*Ir(III)(CO)Cl system and its potential to guide the development of novel iridium-catalyzed cross-coupling methodologies.

Discussion

In conclusion, we have conducted the synthesis and reactivity investigation of acyclic aryl Cp*Ir(III)(CO)Cl species and their transmetallated derivatives, emphasizing three fundamental events: iridation, transmetallation, and electrochemical reductive elimination. Notably, we achieved a well-orchestrated combination of two elementary processes, transmetallation and reductive elimination, between aryl Cp*Ir(III)(CO)Cl species and aryl boronic acids, forming formal Suzuki-Miyaura cross-coupling products in one-pot. Furthermore, these stoichiometric studies inspired the development of a Cp*Ir(III)-catalyzed decarbonylative C–O cross-coupling of aryl aldehydes with carboxylic acids. Overall, this work not only advances the understanding of organoiridium(III) chemistry but also establishes the potential of Cp*Ir(III) complexes as versatile platforms for cross-coupling reactions. We anticipate that these findings will pave the way for further innovations in iridium(III)-enabled catalysis.

Methods

General procedure for the iridation of aryl aldehydes

A flame-dried Schlenk test tube with a magnetic stirring bar was charged with aryl aldehydes (0.40 mmol), $[Cp^*IrCl_2]_2$ (40.0 mg, 0.05 mmol), NaOAc (82.0 mg, 1.0 mmol) and 1,2-dichloroethane (1.0 mL). The reaction mixture was allowed to stir for 5 min at room temperature under a N_2 atmosphere, and then heated at 80 °C in a pre-heated oil bath for 24 h. The reaction mixture was then cooled to room temperature, diluted with 10.0 mL of dichloromethane, filtered through a celite pad, and washed with 25.0–35.0 mL of dichloromethane. The combined organic extracts were concentrated under reduced pressure and the resulting residue was purified by column chromatography on silica gel to provide the desired product.

Data availability

The experimental data generated in this study are provided in the Supplementary Information and Source Data file, and also are available from the corresponding author upon request. Crystallographic data for the structures reported in this article have been deposited at the Cambridge Crystallographic Data Centre (CCDC), under deposition number CCDC 2349028 (**3d**), 2349029 (**3e**), 2349030 (**3f**), 2349031 (**3i**), 2349032 (**3l**), 2349033 (**3w**), 2349034 (**5e**), 2349035 (**5k**), 2349036 (**5p**), 2349037 (**5s**), 2349038 (**5y**), and 2378258 (**6i**). These data can be obtained free of charge via www.ccdc.cam.ac.uk/data_request/cif. Source data are provided with this paper Source data are provided with this paper.

References

1. Kang, J. W., Moseley, K. & Maitlis, P. M. Pentamethylcyclopentadienylrhodium and -iridium halides. I. Synthesis and properties. *J. Am. Chem. Soc.* **91**, 5970–5977 (1969).
2. Kisenyi, J. M. et. al. The cyclometallation of benzoic acid to give rhodium, iridium, and osmium C,O-benzoates. X-ray structure determination of the dibenzoater $[(C_5Me_5)Rh(OOCPh)_2(H_2O)]$. *J. Chem. Soc. Dalton Trans.* **10**, 2459–2466 (1987).
3. Albrecht, M. Cyclometalation using d-block transition metals: fundamental aspects and recent trends. *Chem. Rev.* **110**, 576–623 (2010).
4. Han, Y.-F. & Jin, G.-X. Cyclometalated [Cp*M(C^X)] (M = Ir, Rh; X = N, C, O, P) complexes. *Chem. Soc. Rev.* **43**, 2799–2823 (2014).
5. Li, L., Brennessel, W. W. & Jones, W. D. An efficient low-temperature route to polycyclic isoquinoline salt synthesis *via* C–H activation with $[Cp^*MCl_2]_2$ (M = Rh, Ir). *J. Am. Chem. Soc.* **130**, 12414–12419 (2008).
6. Kim, H., Shin, K. & Chang, S. Iridium-catalyzed C–H amination with anilines at room temperature: compatibility of iridacycles with external oxidants. *J. Am. Chem. Soc.* **136**, 5904–5907 (2014).
7. Hwang, H., Kim, J., Jeong, J. & Chang, S. Regioselective introduction of heteroatoms at the C-8 Position of quinoline *N*-oxides: remote C –H activation using *N*-oxide as a stepping stone. *J. Am. Chem. Soc.* **136**, 10770–10776 (2014).
8. Park, Y., Heo, J., Baik, M.-H. & Chang, S. Why is the Ir(III)-mediated amido transfer much faster than the Rh(III)-mediated reaction? A combined experimental and computational study. *J. Am. Chem. Soc.* **138**, 14020–14029 (2016).
9. Shin, K., Park, Y., Baik, M.-H. & Chang, S. Iridium-catalysed arylation of C–H bonds enabled by oxidatively induced reductive elimination. *Nat. Chem.* **10**, 218–224 (2018).
10. Romanov-Michailidis, F., Ravetz, B. D., Paley, D. W. & Rovis, T. Ir(III)-catalyzed carbocarbation of alkynes through undirected double C–H bond activation of anisoles. *J. Am. Chem. Soc.* **140**, 5370–5374 (2018).
11. Au, Y. K., Lyu, H., Quan, Y. & Xie, Z. Catalytic cascade dehydrogenative cross-coupling of BH/CH and BH/NH: One-pot process to carboranoisoquinolinone. *J. Am. Chem. Soc.* **141**, 12855–12862 (2019).

12. Wang, F., Zhang, L., Han, W., Bin, Z. & You, J. Intramolecular C–H activation as an easy toolbox to synthesize pyridine-fused bipolar hosts for blue organic light-emitting diodes. *Angew. Chem. Int. Ed.* **61**, e202205380 (2022).
13. Jung, H. et al. Photoinduced group transposition *via* iridium-nitrenoid leading to amidative inner-sphere aryl migration. *Angew. Chem. Int. Ed.* **63**, e202408123 (2024).
14. Chen, Z., Kacmaz, A. & Xiao, J. Recent development in the synthesis and catalytic application of iridacycles. *Chem. Rec.* **21**, 1506–1534 (2021).
15. Michon, C., MacIntyre, K., Corre, Y. & Agbossou-Niedercorn, F. Pentamethylcyclopentadienyl iridium(III) metallacycles applied to homogeneous catalysis for fine chemical synthesis. *ChemCatChem* **8**, 1755–1762 (2016).
16. Wang, C. & Xiao, J. Iridacycles for hydrogenation and dehydrogenation reactions. *Chem. Commun.* **53**, 3399–3411 (2017).
17. Woźniak, L. et al. Catalytic enantioselective functionalizations of C–H bonds by chiral iridium complexes. *Chem. Rev.* **120**, 10516–10543 (2020).
18. Li, X. et al. Recent development on Cp*Ir(III)-catalyzed C–H bond functionalization. *ChemCatChem* **12**, 2358–2384 (2020).
19. Hong, S. Y. et al. Selective formation of γ-lactams *via* C–H amidation enabled by tailored iridium catalysts. *Science* **359**, 1016–1021 (2018).
20. Wang, H. et al. Iridium-catalyzed enantioselective C(sp^3)–H amidation controlled by attractive noncovalent interactions. *J. Am. Chem. Soc.* **141**, 7194–7201 (2019).
21. Hong, S. Y., Kim, D. & Chang, S. Catalytic access to carbocation intermediates *via* nitrenoid transfer leading to allylic lactams. *Nat. Catal.* **4**, 79–88 (2021).
22. Mas-Roselló, J. et al. Iridium-catalyzed acid-assisted hydrogenation of oximes to hydroxylamines. *Angew. Chem. Int. Ed.* **60**, 15524–15532 (2021).
23. Gao, Y. et al. Additive-free transfer hydrogenative direct asymmetric reductive amination using a chiral pyridine-derived half-sandwich catalyst. *Angew. Chem. Int. Ed.* **62**, e202303709 (2023).
24. Qi, L.-W., Rogge, T., Houk, K. N. & Lu, Y. Iridium nitrenoid-enabled arene C–H functionalization. *Nat. Catal.* **7**, 934–943 (2024).
25. Lin, Y., Xu, G. & Tang, W. Chiral polymeric diamine ligands for iridium-catalyzed asymmetric transfer hydrogenation. *J. Am. Chem. Soc.* **146**, 27736–27744 (2024).
26. Kang, J. W. & Maitlis, P. M. Pentamethycyclopentadienyl)rhodium and –iridium complexes IV. Oxidative additions to dicarbonyl(pentamethylcyclopentadienyl) rhodium and –iridium. *J. Organometal. Chem.* **26**, 393–399 (1971).
27. Janowicz, A. H. & Bergman, R. G. C–H activation in completely saturated hydrocarbons: Direct observation of M + R–H → M(R)(H). *J. Am. Chem. Soc.* **104**, 352–354 (1982).
28. Hoyano, J. K. & Graham, W. A. G. Oxidative addition of the carbon-hydrogen bonds of neopentane and cyclohexane to a photochemically generated iridium(I) complex. *J. Am. Chem. Soc.* **104**, 3723–3725 (1982).
29. Gómez, M., Yarrow, P. I. W., Robinson, D. J. & Maitlis, P. M. A new aromatic metalation reaction involving rhodium and iridium; the unusual reactivity of iodobenzene. *J. Organometal. Chem.* **279**, 115–130 (1985).
30. Arndtsen, B. A. & Bergman, R. G. Unusually mild and selective hydrocarbon C–H bond activation with positively charged iridium(III) complexes. *Science* **270**, 1970–1973 (1995).
31. Alaimo, P. J., Arndtsen, B. A. & Bergman, R. G. Synthesis of tertiary and other sterically demanding alkyl and aryl complexes of iridium by aldehyde C–H bond activation. *J. Am. Chem. Soc.* **119**, 5269–5270 (1997).
32. Hughes, R. P. et al. Iridium and rhodium complexes containing fluorinated phenyl ligands and their transformation to η^2-benzyne complexes, including the parent benzyne complex IrCp*(PMe_3)(C_6H_4). *Organometallics* **21**, 4873–4885 (2002).
33. Bergman, R. G. Activation of alkanes with organotransition metal complexes. *Science* **223**, 902–908 (1984).
34. Sridevi, V. S., Fan, W. Y. & Leong, W. K. Cp*$IrCl_2]_2$-assisted C≡C bond cleavage with water: An experimental and computational study. *Organometallics* **26**, 1173–1177 (2007).
35. Meredith, J. M., Robinson, R. Jr., Goldberg, K. I., Kaminsky, W. & Heinekey, D. M. C–H bond activation by cationic iridium(III) NHC complexes: a combined experimental and computational study. *Organometallics* **31**, 1879–1887 (2012).
36. Frasco, D. A. et al. Nondirected C–H activation of arenes with Cp*Ir(III) acetate complexes: An experimental and computational study. *Organometallics* **35**, 2435–2445 (2016).
37. Tellers, D. M., Yung, C. M., Arndtsen, B. A., Adamson, D. R. & Bergman, R. G. Electronic and medium effects on the rate of arene C–H bond activation by cationic Ir(III) complexes. *J. Am. Chem. Soc.* **124**, 1400–1410 (2002).
38. Cordaro, J. G. & Bergman, R. G. Dissociation of carbanions from acyl iridium compounds: an experimental and computational investigation. *J. Am. Chem. Soc.* **126**, 16912–16929 (2004).
39. Kawahara, R., Fujita, K.-I. & Yamaguchi, R. Multialkylation of aqueous ammonia with alcohols catalyzed by water-soluble Cp*Ir-ammine complexes. *J. Am. Chem. Soc.* **132**, 15108–15111 (2010).
40. Lee, J. Y., Fan, W. Y., Mak, K. H. G. & Leong, W. K. The formation of aldehydes from the photochemically activated reaction of Cp*Ir(CO)(Cl)(CH_2R) complexes with water. *J. Organometal. Chem.* **724**, 275–280 (2013).
41. Tan, G., You, Q. & You, J. Iridium-catalyzed oxidative heteroarylation of arenes and alkenes: Overcoming the restriction to specific substrates. *ACS Catal.* **8**, 8709–8714 (2018).
42. Lapointe, D. & Fagnou, K. Overview of the mechanistic work on the concerted metallation deprotonation pathway. *Chem. Lett.* **39**, 1118–1126 (2010).
43. Hartwig, J. F. *Organotransition Metal Chemistry, From Bonding to Catalysis*. (University Science Books, 2010).
44. Liu, J., Wu, X., Iggo, J. A. & Xiao, J. Half-sandwich iridium complexes—synthesis and applications in catalysis. *Coord. Chem. Rev.* **252**, 782–809 (2008).
45. Spessard, G. O. & Miessler, G. L. *Organometallic Chemistry*. (Oxford University Press: New York, 2010).
46. Rasmussen, S. C. Transmetalation: a fundamental organometallic reaction critical to synthesis and catalysis. *ChemTexts.* **7**, 1–8 (2021).
47. Chinchilla, R. & Nájera, C. The Sonogashira reaction: a booming methodology in synthetic organic chemistry. *Chem. Rev.* **107**, 874–922 (2007).
48. Colacot, T. *New Trends in Cross-Coupling: Theory and Applications*. (The Royal Society of Chemistry, Cambridge, 2015).
49. Miyaura, N. & Suzuki, A. Palladium-catalyzed cross-coupling reactions of organoboron compounds. *Chem. Rev.* **95**, 2457–2483 (1995).
50. Seechurn, C. C. C. J., Kitching, M. O., Colacot, T. J. & Snieckus, V. Palladium-catalyzed cross-coupling: A historical contextual perspective to the 2010 Nobel Prize. *Angew. Chem. Int. Ed.* **51**, 5062–5085 (2012).
51. Ruiz-Castillo, P. & Buchwald, S. L. Applications of palladium-catalyzed C–N cross-coupling reactions. *Chem. Rev.* **116**, 12564–12649 (2016).
52. Biffis, A., Centomo, P., Zotto, A. D. & Zecca, M. Pd metal catalysts for cross-couplings and related reactions in the 21st century: a critical review. *Chem. Rev.* **118**, 2249–2295 (2018).
53. Hassan, J., Sévignon, M., Gozzi, C., Schulz, E. & Lemaire, M. Aryl-aryl bond formation one century after the discovery of the Ullmann reaction. *Chem. Rev.* **102**, 1359–1469 (2002).

54. Evano, G., Blanchard, N. & Toumi, M. Copper-mediated coupling reactions and their applications in natural products and designed biomolecules synthesis. *Chem. Rev.* **108**, 3054–3131 (2008).
55. Qiao, J. X. & Lam, P. Y. S. "Recent advances in Chan–Lam coupling reaction: copper-promoted C–heteroatom bond cross-coupling reactions with boronic acids and derivatives". *Boronic Acids: Preparation and Applications in Organic Synthesis, Medicine and Materials* (Wiley-VCH.) 315–361 (2011).
56. Rosen, B. M. et al. Nickel-catalyzed cross-couplings involving carbon-oxygen bonds. *Chem. Rev.* **111**, 1346–1416 (2011).
57. Tasker, S. Z., Standley, E. A. & Jamison, T. F. Base-free nickel-catalysed decarbonylative Suzuki–Miyaura coupling of acid fluorides. *Nature* **563**, 100–104 (2018).
58. Zubaydi, S. A. et al. Reductive alkyl-alkyl coupling from isolable nickel-alkyl complexes. *Nature* **634**, 585–591 (2024).
59. Dinh, L. P. et al. Persistent organonickel complexes as general platforms for Csp^2–Csp^3 coupling reactions. *Nat. Chem.* **16**, 1515–1522 (2024).
60. Cahiez, G. & Moyeux, A. Cobalt-catalyzed cross-coupling reactions. *Chem. Rev.* **110**, 1435–1462 (2010).
61. Corbet, J.-P. & Mignani, G. Selected patented cross-coupling reaction technologies. *Chem. Rev.* **106**, 2651–2710 (2006).
62. Jana, R., Pathak, T. P. & Sigman, M. S. Advances in transition metal (Pd,Ni,Fe)-catalyzed cross-coupling reactions using alkyl-organometallics as reaction partners. *Chem. Rev.* **111**, 1417–1492 (2011).
63. Korch, K. M. & Watson, D. A. Cross-coupling of heteroatomic electrophiles. *Chem. Rev.* **119**, 8192–8228 (2019).
64. Camasso, N. M. & Sanford, M. S. Design, synthesis, and carbon-heteroatom coupling reactions of organometallic nickel(IV) complexes. *Science* **347**, 1218–1220 (2015).
65. Kim, J., Shin, K., Jin, S., Kim, D. & Chang, S. Oxidatively induced reductive elimination: exploring the scope and catalyst systems with Ir, Rh, and Ru complexes. *J. Am. Chem. Soc.* **141**, 4137–4146 (2019).
66. Hansch, C., Leo, A. & Taft, R. W. Survey of Hammett substituent constants and resonance and field parameters. *Chem. Rev.* **91**, 165–195 (1991).
67. Sandford, C. et al. A synthetic chemist's guide to electroanalytical tools for studying reaction mechanisms. *Chem. Sci.* **10**, 6404–6422 (2019).
68. Robinson, S. G. & Sigman, M. S. Integrating electrochemical and statistical analysis tools for molecular design and mechanistic understanding. *Acc. Chem. Res.* **53**, 289–299 (2020).
69. Rafiee, M. et al. Cyclic Voltammetry and chronoamperometry: mechanistic tools for organic electrosynthesis. *Chem. Soc. Rev.* **53**, 566–585 (2024).
70. Leech, M. C. & Lam, K. A practical guide to electrosynthesis. *Nat. Rev. Chem.* **6**, 275–286 (2022).
71. Yuan, Y., Yang, J. & Lei, A. Recent advances in electrochemical oxidative cross-coupling with hydrogen evolution involving radicals. *Chem. Soc. Rev.* **50**, 10058–10086 (2021).
72. Malapit, C. A. et al. Advances on the merger of electrochemistry and transition metal catalysis for organic synthesis. *Chem. Rev.* **122**, 3180–3218 (2022).
73. Wang, Y. et al. Electrochemical late-stage functionalization. *Chem. Rev.* **123**, 11269–11335 (2023).
74. Hamby, T. B., LaLama, M. J. & Sevov, C. S. Controlling Ni redox states by dynamic ligand exchange for electroreductive Csp^3–Csp^2 coupling. *Science* **376**, 410–416 (2022).
75. Das, D., Dinh, L. P., Smith, R. E., Kalyani, D. & Sevov, C. S. Nickel-mediated aerobic $C(sp^2)$–nucleophile coupling reactions for late-stage diversification of aryl electrophiles. *Nat. Catal.* **7**, 934–943 (2024).
76. Connelly, N. G. & Geiger, W. E. Chemical redox agents for organometallic chemistry. *Chem. Rev.* **96**, 877–910 (1996).

Acknowledgements

We acknowledge financial support from the National Natural Science Foundation of China (No. 22031007, J.Y., 22401200, G.T.), and the Fundamental Research Funds for the Central Universities (YJ202340, G.T.). We thank the support from the Analytical and Testing Center of Sichuan University and Dr. J. Li, Dr. M. Yang, and Dr. C. Wang from Comprehensive Training Platform Specialized Laboratory, College of Chemistry, Sichuan University. We also thank Prof. T.-S. Mei from Shanghai Institute of Organic Chemistry, Chinese Academy of Sciences for discussions regarding electrochemistry.

Author contributions

G.T. performed initial exploratory experiments. Y.W. and Y.D. performed synthetic experiments and computations. J.Y. and G.T. designed and directed the project. Y.W., G.T. and J.Y. wrote the paper. All authors contributed to discussions.

Competing interests

The authors declare no competing interests.

Additional information

Supplementary information The online version contains supplementary material available at https://doi.org/10.1038/s41467-025-59817-9.

Correspondence and requests for materials should be addressed to Guangying Tan or Jingsong You.

Peer review information *Nature Communications* thanks the anonymous reviewer(s) for their contribution to the peer review of this work. A peer review file is available.